Experimental orthotopic transplantation of a tissue-engineered oesophagus in rats.

Sebastian Sjoqvist, Philipp Jungebluth, Mei Ling Lim, Johannes C. Haag, Ylva Gustafsson, Greg Lemon, Silvia Baiguera, Miguel Angel Burguillos, Costantino Del Gaudio, Oscar E. Simonsson, Antonio Beltran Rodriguez, Alexander Sotnichenko, Karolina Kublickiene, Henrik Ullman, Heike Kielstein, Peter Damberg, Alessandra Bianco, Rainer Heuchel, Ying Zhao, Domenico Ribatti, Cristian Ibarra, Bertrand Joseph, Doris A. Taylor & Paolo Macchiarini.

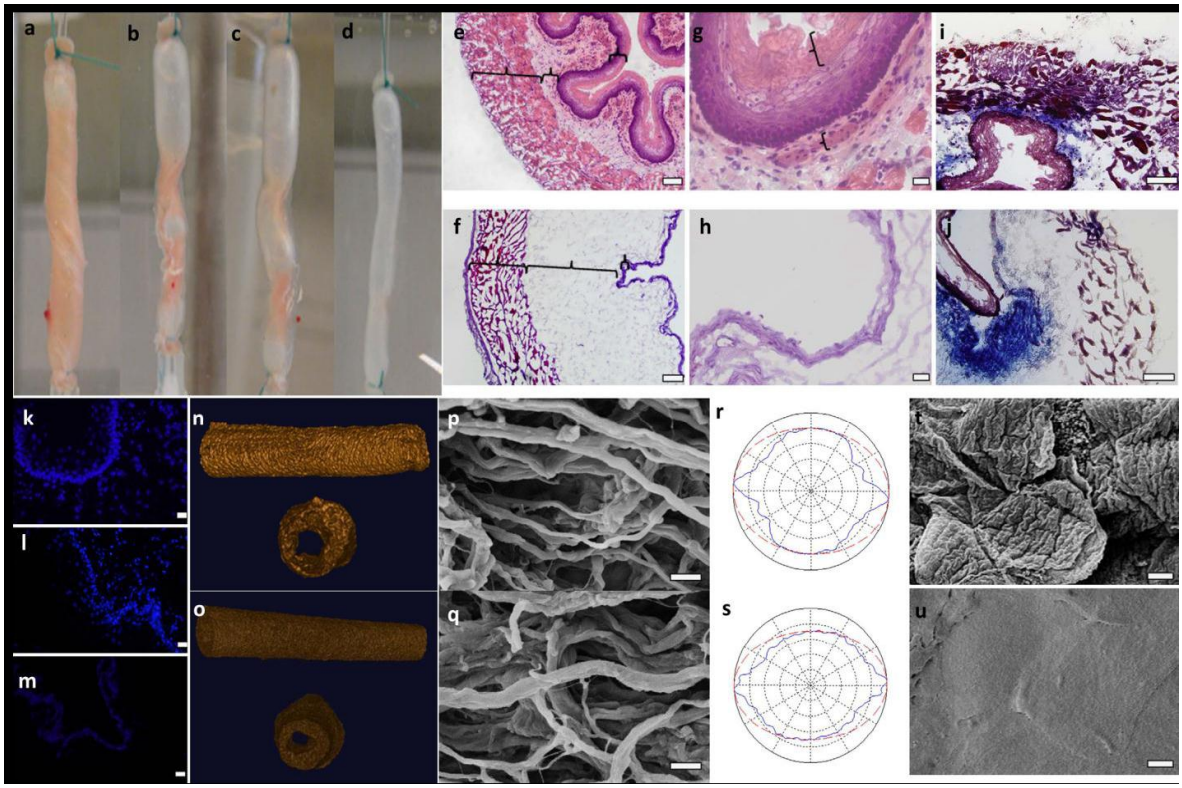

Figure 1 | Gross appearance and architectural evaluation of decellularized oesophagus. (a–d) Gross morphology of the oesophagus after perfusion decellularization process at 0 (a), 30 (b), 60 (c) and 120 min (d). (e–h) Haematoxylin and eosin staining showing mucosa (m), submucosa (sm), muscularis externa (mu) and lumen (l) in native (e,g) and decelluarized (f,h) oesophagus (scale bar—100 mm). Higher magnification of the mucosa showing lumen (l), keratin (k) and muscularis mucosa (mm) of native oesophagus (g; scale bar—20 mm). No cell nuclei or keratin are visible in the mucosa of decellularized oesophagus, lumen is marked (l) (h). (i,j) Masson's trichrome staining of native (i) and decellularized (j) oesophagus, showing the retention of collagen (blue) in the submucosa (scale bar—100 mm). (k–m) 4DAPI showing cell nuclei in a multilayered configuration close to the lumen (l)in native (k) and decellularized using agitation (l) oesophagus, while in the perfusion group (m) the staining is weaker, smeared and without any intact cell nuclei (scale bar—50 mm). (n,o)Micro CT scan of native (n) and decellularized (o) oesophagus. (p–u) SEM evaluations of external side of native (p) and decellularized (q) oesophagus (scale bar—5 mm). Computer-based fibre evaluation showing the similarity of orientation between native (r) and decellularized oesophagus (s), blue line: computed pattern representative of fibre orientation. Red line: fitting ellipse of the computed pattern. SEM ofluminal surface of the native oesophagus with flattened, cuboidal epithelial cells (t) and decellularized oesophagus showing a smooth basement membrane. (u; scale bar—4 mm).

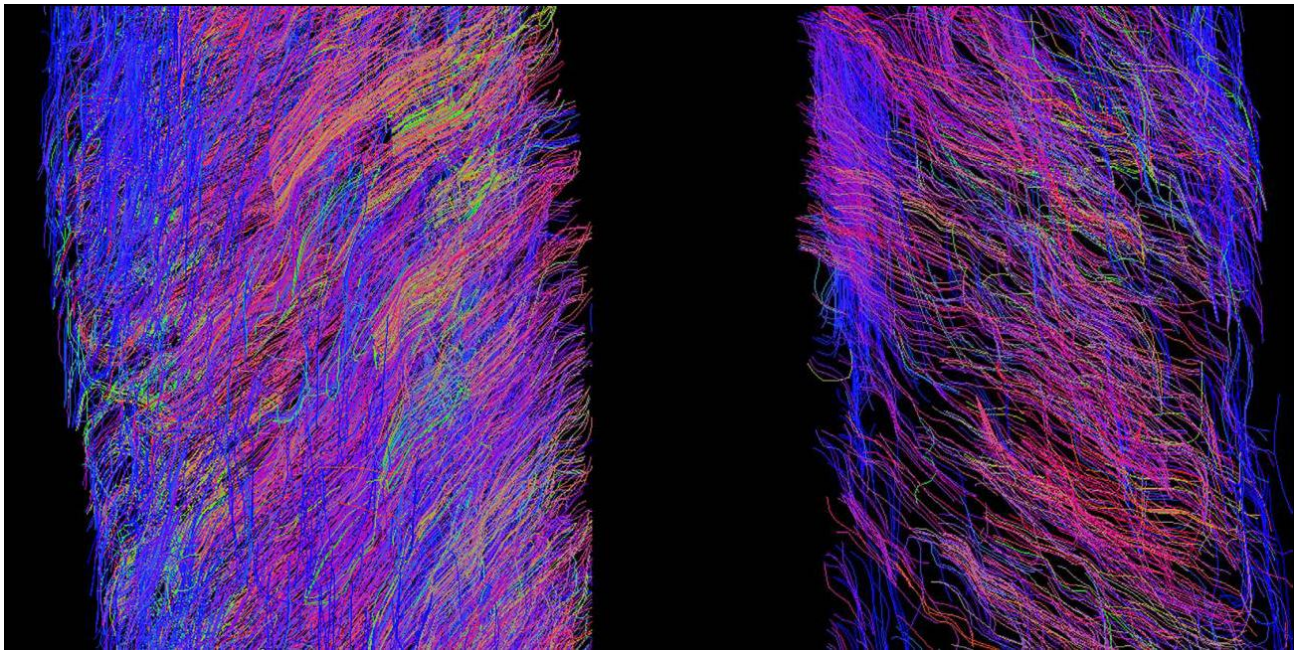

Figure 2 | Tractography evaluation. Tractography based on diffusion tensor imaging of native (left) and decellularized (right) rat oesophagus. The general fibre orientations are maintained but fewer tracts were detected in the decellularized sample.

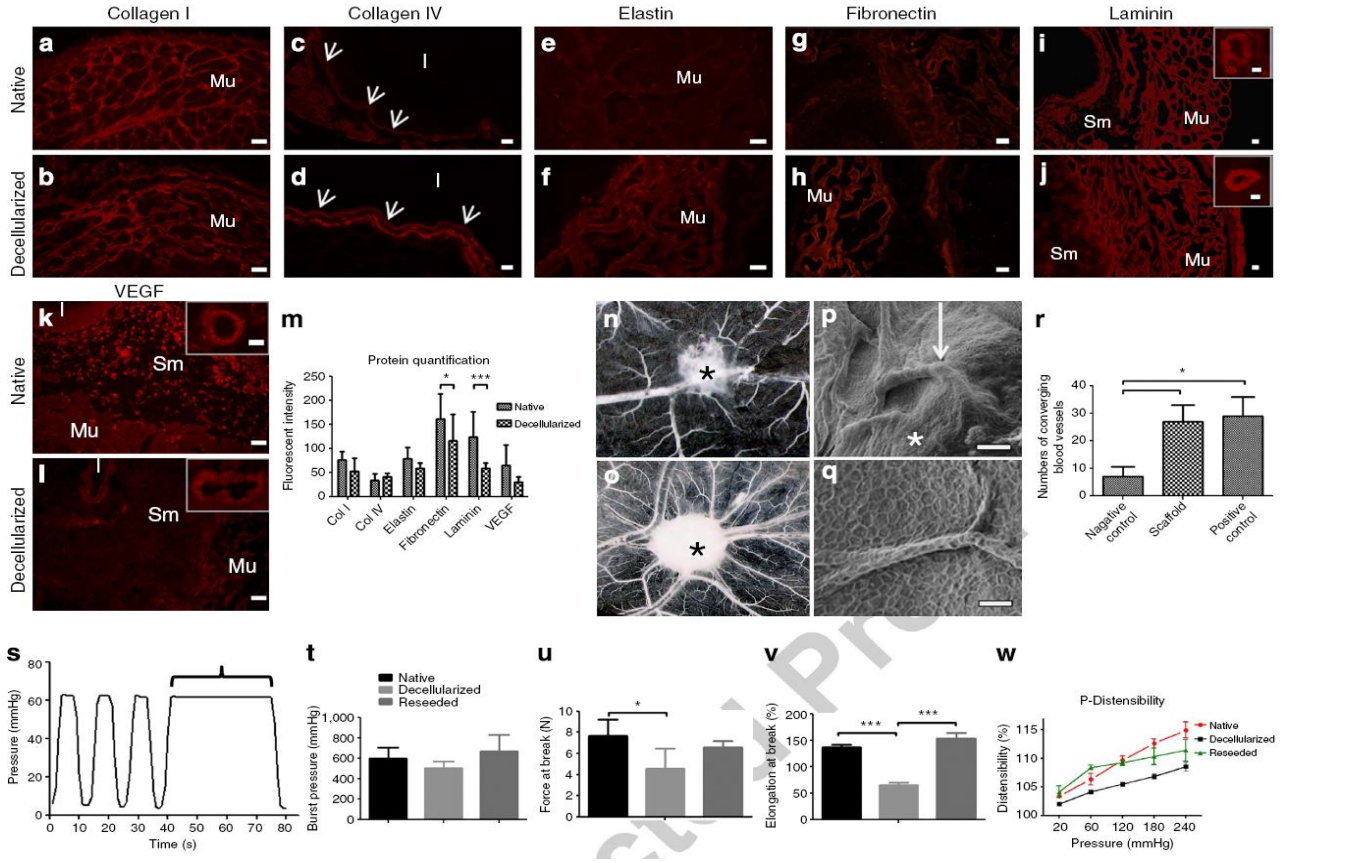

Figure 3 | Protein content and functional assays. (a–d) Expression of collagen I and IV in native (a,c) and decellularized (b,d) oesophagus (scale bar—Col I—50 mm, Col IV—20mm, mu indicating muscular layer, l—lumen). An intact basement membrane is indicated by collagen IV expression (c,d, red arrows). (e–j) Expression of elastin, fibronectin and laminin in native (e,g,i, mu indicating muscular layer, sm submucosa) and decellularized (f,h,j) oesophagus (scale bar—25 mm). (k,l) Expression of VEGF factor in native (k) and decellularized (l) oesophagus (l—lumen, sm—submucosa, mu—muscular layer). VEGF-stained tubular structures, suggesting intact vasculature, are found in native and decellularized tissue (i–l, inserts, scale bar—10 mm). (m) Protein quantification of extracellular matrix proteins (nj3 biological replicates). (n–q) Angiogenesis assay implanted with gelfoam (control, asterisk in n) and Q11 with fragments of decellularized oesophagus (asterisk in o). The oesophagus induced new vessels, proving the scaffolds' positive influence of vessel organization. SEM micrographs of vessel and the scaffold sample (p, *) and newly built vessel (p, k) (scale bar—100 mm), higher magnification on one of the vessels(q; scale bar—25 mm). (r) Quantification of blood vessels converging to the samples, indicating the strong angiogenic induction by the scaffold, at the levels of the positive control (nj3). (s) The scaffold was inflated and deflated over 10,000 times, a stable plateau phase (s, arrow heads) proves the scaffold's integrity in the last cycle, as there is no leakage from the scaffold (nj3, one representative graph shown). (t) Axial strength was evaluated using burst pressure measurements, without any difference between native, decellularized or reseeded groups (nj5). (u,v) Tensile test showed that strength lost during decellularization was regained after reseeding, force at break (u) and strain at break (v) (nj5). (w) Distensibility assay showed that the lost distensibility after decellularization (black series) was regained after reseeding (green series) (nj5). *Po0.05, **Po0.01, ***Po0.001 by analysis of variance (ANOVA) followed by Tukey's post hoc tests for (r,u,v), or ANOVA followed by Bonferroni post tests for (m,w).

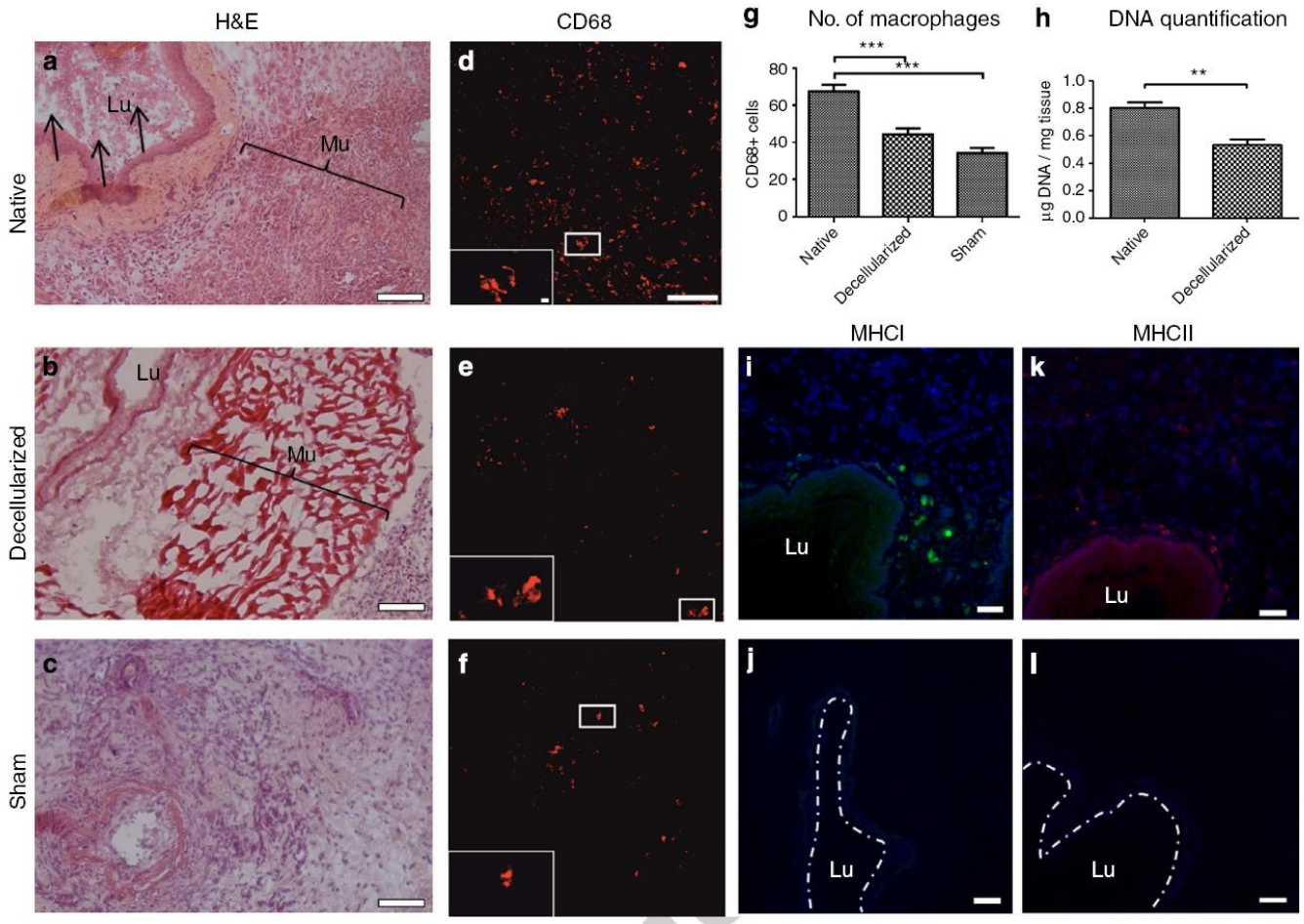

Figure 4 | Immunogenic properties of the scaffold. (a–c) Histology from 5-day subcutaneous transplantations of native, decellularized oesophagus and sham surgery (scale bar—100 mm). The native organ was heavily infiltrated with host cells resulting in almost complete destruction of the graft. The muscular layer shows almost total degradation (a, bracket) and the lumen (a, lu) has been invaded by cells (a, arrowhead). In contrast, the decellularized organ has an intact muscular layer (b, bracket) and fewer infiltrating cells. The scaffold's integrity also appeared intact as no cells were invading to the lumen (b, lu marks lumen, mu muscular layer). The sham surgery (c) showed similar inflammatory response as the decellularized group. (d–f) Macrophages in the subcutaneous implantation groups were stained and quantified. There was a considerable increase in CD68ю cells in the native, allotransplantation (d) as compared with both decellularized organ (e) and sham surgery groups (skin incision) (f) (scale bar—67 mm, insert scale bars—11 mm). (g) Quantification of number of macrophages in each group, showed differences between native group and the other two, but no difference between decellularized oesophagus and sham groups (nj3). (h) The DNA content in the decellularized organ was moderately decreased compared with the native organ. (i–l) Major histocompatibility complexes I- and II-positive cells were totally eliminated in decellularized oesophagus (j,l) compared with native oesophagus (i,k) (scale bar—50 mm). ***Po0.001 by ANOVA followed by Tukey's post hoc tests for (g). **Po0.001 by Student's t-test for (h).

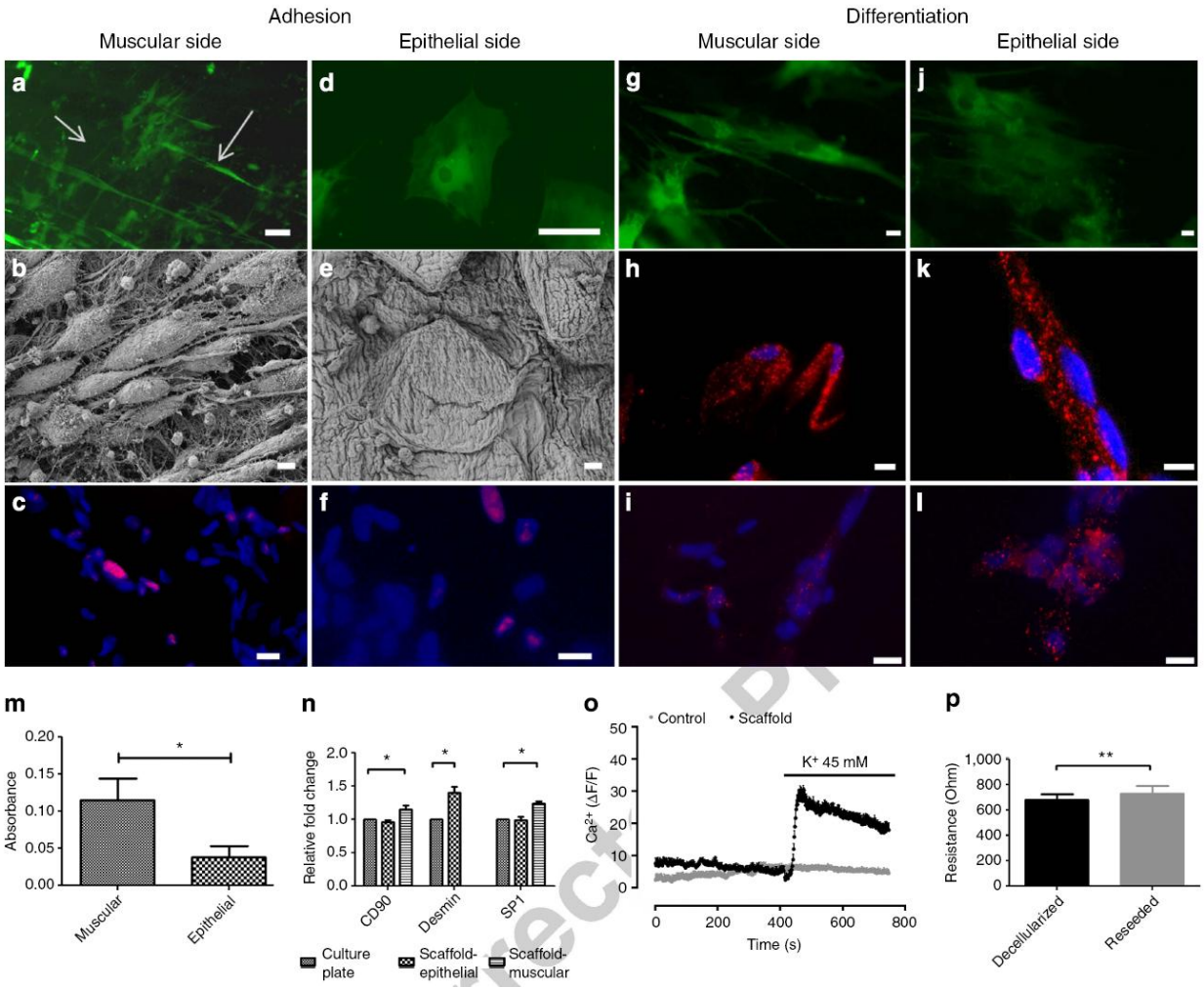

Figure 5 | Cell-scaffold interaction. (a) GFP-positive cells on the muscular side of the scaffold showed an elongated morphology 48 h after seeding, with cells aligned in two main orientations (arrows), which corresponded to the directions of muscular layer's fibres (scale bar—50 mm). (b) SEM image confirmed the cell morphology (scale bar—5 mm). (c) Ki-67 (red) proved the presence of proliferative cells on scaffold (nuclei counterstained with DAPI, scale bar—50 mm). (d,e) Cells seeded to the epithelial side of the scaffold had a cuboidal shape (d, green—GFP, scale bar—50 mm), further confirmed by SEM (e, scale bar—5 mm). (f) Ki-67 showed the presence of proliferative cells on the epithelial layer (scale bar—50 mm). (g–i) After 3-week culture, the cells on the muscular side retained the elongated morphology (g) and stained positive for muscular markers myoD1 (h) and desmin (i) (green—GFP, markers red, nuclei stain DAPI (blue) scale bar—10 mm). (j–l) Cells grown on the epithelial side for 3 weeks showed cuboidal morphology and were positive for epithelial markers pan-keratin (k) and tight junction protein zona occludens-2 (l) (green—GFP, markers red, nuclei-stained DAPI (blue) scale bar—10 mm). (m) 3-(4,5-dimethylthiazol-2-yl)-2,5-diphenyltetrazolium bromide assay proved that the cells were metabolically active on the scaffold (nj3). (n) rtPCR showed that the cells retained their MSC marker CD90 but had different gene expression for muscular (desmin) and epithelial (sp1) differentiation markers depending on location of growth (nj3). (o) Cells grown on either culture plates or cryosections of the decellularized scaffolds for 3 weeks were loaded with a calcium dye and tested for calcium fluxation. Elevation of extracellular Kю concentration triggered calcium transients only in cells grown on the cryosection (scaffold) in contrast to the cells grown on culture dish (control). (p) The decellularized mucosa's electrical resistance showed a small but significant increase after reseeding and culturing for 3 weeks (nj3). *Po0.05 by ANOVA followed by Tukey's post hoc tests for (n). *Po0.05, **Po0.01 by unpaired (m) and paired (p) Student's t-test.

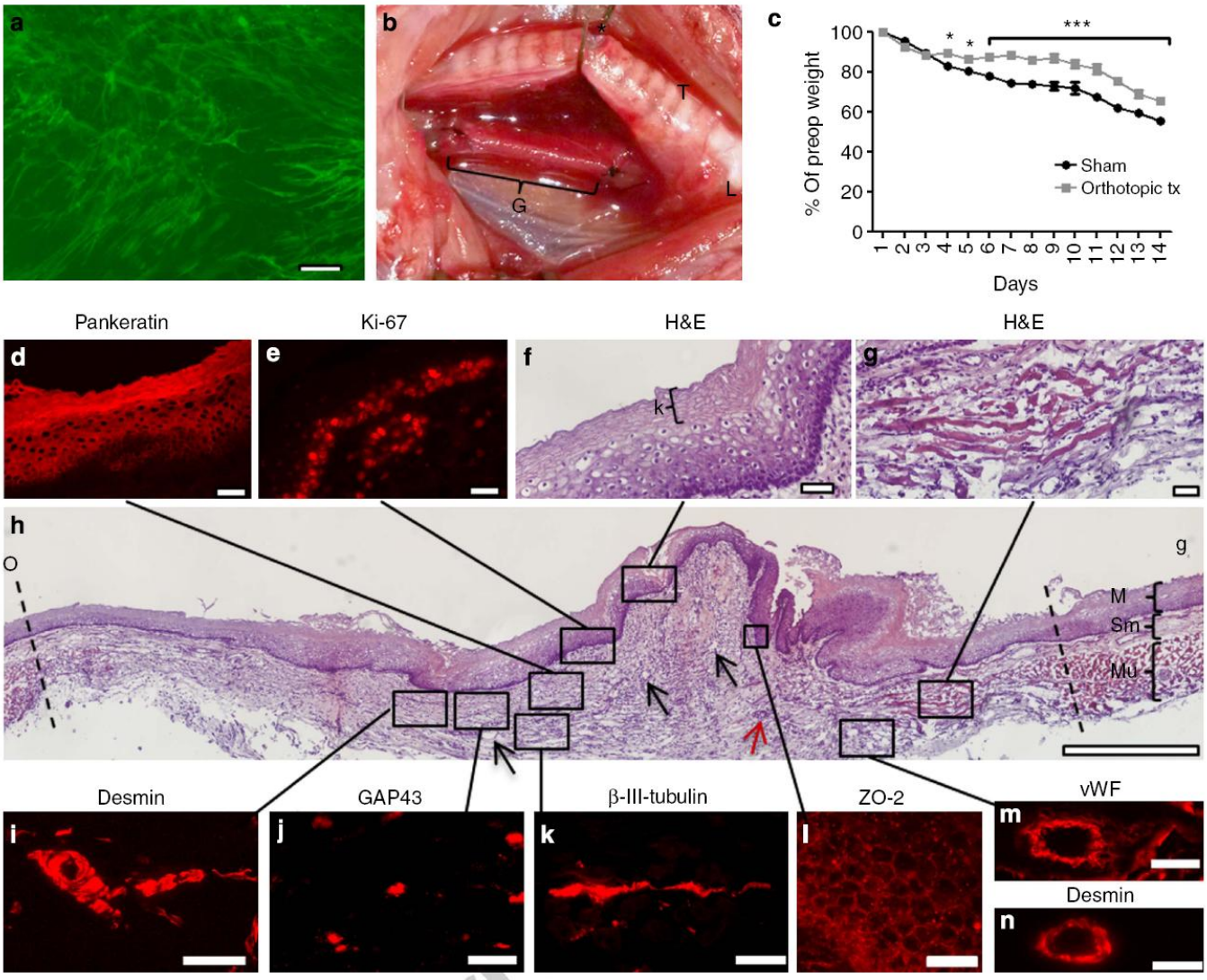

Figure 6 | Fourteen-day orthotopic transplantation. (a) GFP-labelled cells after 3 weeks' culture on tubular scaffold (scale bar—50 mm). (b) Orthotopic replacement of the entire cervical oesophagus with a reseeded tissue-engineered graft (g), the trachea (t) was partially opened (*) to facilitate breathing, the lower part of the larynx is observed (l). (c) Postoperative weight curves. The animals receiving tissue-engineered grafts lost weight in lesser extent to control surgery and weight gain was observed at some time points (* indicate significance levels between the groups). (d) The neo-epithelium stained positively for pankeratin (scale bar—50 mm). (e) Proliferative cells were found in the basal part of the epithelium (scale bar—20mm). (f) High
power magnification showed a seven- to nine-layer thick epithelium with a superficial keratin layer (f,k; scale bar—50 mm). (g) High power magnification of regenerated muscle fibres (scale bar—50 mm). (h) Sagittal section of the oesophageal wall, the whole graft (marked with dashed lines) was re-epithelized, several blood vessels (black arrows), a few accumulations of inflammatory cells (red arrow) were found. (scale bar—500 mm. m indicates mucosa, sm submucosa, mu muscular layer, o and g indicate oral and gastric sides of the explant). (i–n) Repopulation of the scaffold of different cell types was proven by immunohistochemistry (scale bars—50 mm, for ZO 2–20 mm); desmin-positive cells were found throughout the graft (i), Gap43 and Beta-III-tubulin-positive staining suggested in-growth of neurons (j,k). Zona occludens-II, a tight junction protein, showed a pattern consistent with a healthy epithelium (l). Potential vasculature stained positively for von willebrand factor (m) out of which some stained positively for desmin (n), suggesting arterioles. *Po0.05, ***Po0.001 by ANOVA followed by Bonferroni post tests for (c).

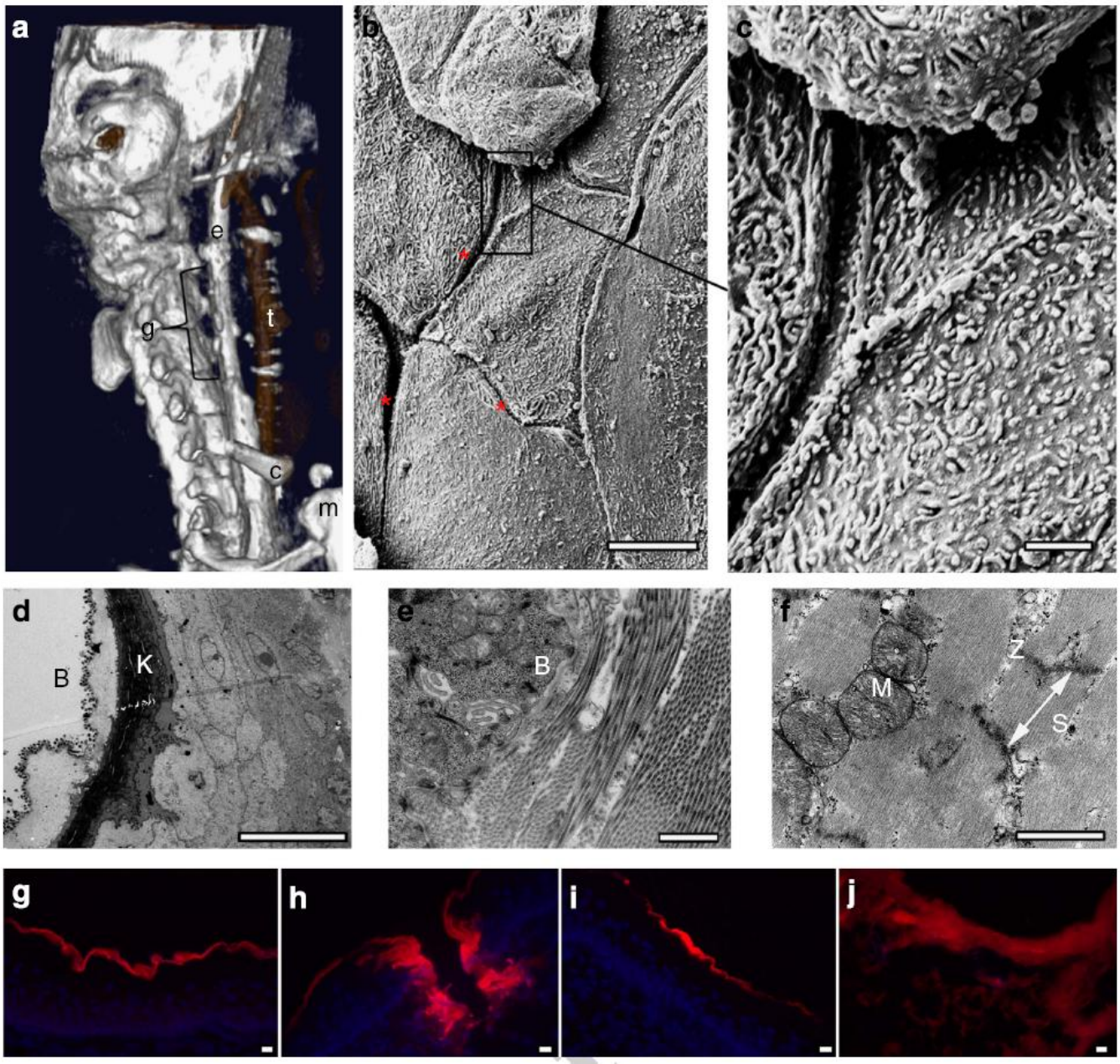

Figure 7 | Imaging and functional assays of in vivo regenerated scaffold. (a) Contrast-enhanced computed tomography showed a smooth and patent oesophagus (bracket), anatomical landmarks: e—oesophagus, t—trachea (air-filled), c—clavicle, m—manubrium. (b,c) SEM of neo-epithelium showed a confluent cell layer with characteristic leaf-like morphology and small intercellular spaces (b, *) (scale bar—10 mm). Higher magnification of epithelial cells showed many folds in the cell membrane indicating a healthy epithelium (c; scale bar—2 mm). (d–f) TEM imaging showed a six- to eight-layered keratinized (d, K) epithelium with bacteria (d, B) only on the luminal side (d, B) (scale bar—10 mm). Aligned collagen fibres were seen underlying the basal membrane (e, B) (scale bar—1 mm). Deeper, muscle bundles were present, with abundant mitochondriae (f, M) and sarcomeres (f, S) bordered by Z-lines (f, Z) (scale bar—1 mm). (g–j) Biotin assay was performed to functionally test the regenerated epithelium. In the native epithelium, the staining was limited to the superficial surface (g), while a mechanically damaged epithelium showed a diffuse staining deeper in the epithelium (h). The regenerated epithelium (i) showed similar staining to the native epithelium. Assay performed on the decellularized scaffold showed a general diffusion through the mucosa to the submucosal (j; scale bar—20 mm).

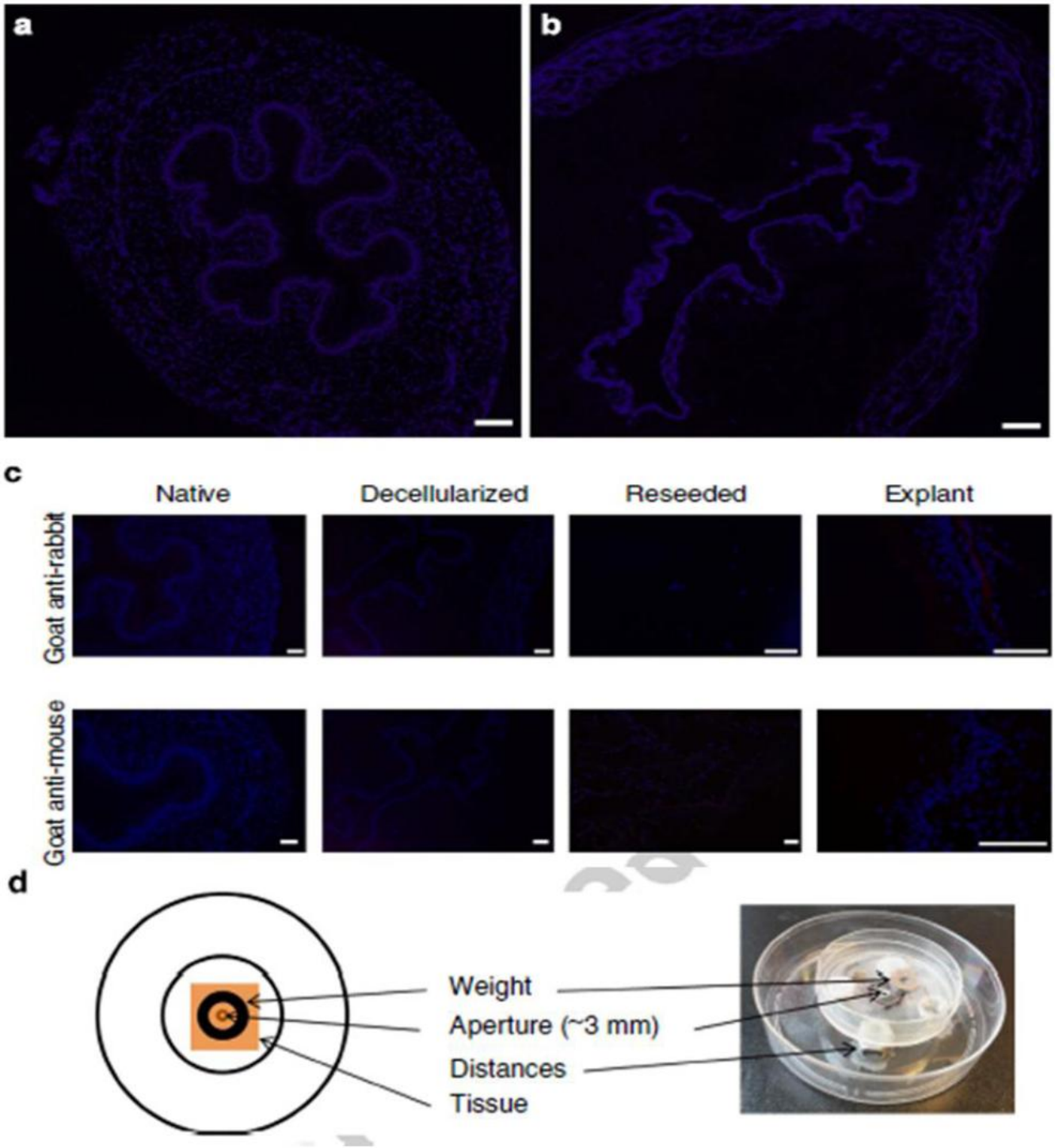

Figure 8 | Control staining and tissue electrical resistance construct. (a,b) Larger images of nuclear staining showed intact cell nuclei in the native oesophagus (a), while the decellularized oesophagus showed a smeared staining, without any intact cell nuclei (b, the intensity of the decellularized sample has been increased to easier identify the localization staining; scale bar—200 mm). (c) Secondary only staining of each representative antibody (scale bar—100 mm). (d) Custom-made construct to mount the tissue for electrical resistance testing. The tissue was separating the PBS in the two different Petri dishes and the electrical resistance between the two dishes was measured.